$s=\frac{1}{2}$ antiferromagnetic Heisenberg model on fullerene-type symmetry clusters

N. P. Konstantinidis
Institut für Theoretische Physik A, Physikzentrum, RWTH Aachen, 52056 Aachen, Germany;
Institut für Festkörperforschung-Theorie III, Forschungszentrum Jülich, Leo-Brandt-Strasse, 52425 Jülich, Germany;
and JARA-Fundamentals of Future Information Technology

(Received 14 June 2009; revised manuscript received 16 September 2009; published 30 October 2009)

The $s_i=\frac{1}{2}$ nearest-neighbor antiferromagnetic Heisenberg model is considered for spins sitting on the vertices of clusters with the connectivity of fullerene molecules and a number of sites n ranging from 24 to 32. Using the permutational and spin-inversion symmetries of the Hamiltonian, the low-energy spectrum is calculated for all the irreducible representations of the symmetry group of each cluster. Frustration and connectivity result in nontrivial low-energy properties, with the lowest excited states being singlets except for $n=28$. Same-hexagon and same-pentagon correlations are the most effective in the minimization of the energy, with the $n=32$ $-D_{3h}$ symmetry cluster having an unusually strong singlet intrapentagon correlation. The magnetization in a field shows no discontinuities unlike the icosahedral I_h fullerene clusters but only plateaux with the most pronounced for $n=28$. The spatial symmetry as well as the connectivity of the clusters appear to be important for the determination of their magnetic properties.

DOI: 10.1103/PhysRevB.80.134427 PACS number(s): 75.10.Jm, 75.50.Ee, 75.50.Xx

I. INTRODUCTION

The antiferromagnetic Heisenberg model (AHM) has been the object of intense investigation for some time now as a prototype of strongly correlated electronic behavior. The effects of frustration, quantum fluctuations, and low dimensionality can lead to new phases differing from conventional order and possessing a nontrivial low-energy spectrum.[1–3] Small magnetic clusters provide an excellent testing ground for the validity of the AHM as well as other theoretical models, as oftentimes its low-energy properties can be computed on these structures and its predictions can be directly tested against experiments.[4]

Here the model is investigated for spins sitting on vertices of fullerene-type clusters. Fullerene molecules superconduct when doped with alkali metals.[5,6] An electronic mechanism for superconductivity was suggested based on perturbation-theory calculations on the one-band Hubbard model on doped C_{60}, the fullerene with 60 carbon atoms. Geometrically it corresponds to the truncated icosahedron and possesses icosahedral I_h point-group symmetry.[7] However, diagonalization of the Hubbard model is prohibitive due to limitations imposed by the dimensionality of the Hilbert space. As a first step, the strong on-site repulsion limit at half filling, the AHM, was considered on clusters of I_h symmetry.[8] Correlations between magnetic properties and spatial symmetry at the classical and quantum levels were found, which pointed to the possibility of studying smaller clusters to gain insight on larger ones of the same symmetry but intractable with present day computational means. This approach could as well be used for the Hubbard model to investigate superconducting correlations.[9] For the I_h-symmetry class, the low-energy spectrum of the AHM can only be calculated for the dodecahedron that has 20 sites,[10] as the next larger I_h cluster is C_{60} which has an enormous Hilbert space even in the AHM case. Here we consider clusters with a number of sites (or vertices) n up to 32, where calculation of the low-energy spectrum is possible. In addition, nearest-neighbor correlation functions and the response in an external magnetic field are computed, quantities that are experimentally accessible should molecules of these type with magnetic properties described by the AHM become available in the laboratory. Correlations between the calculated quantities and spatial symmetry and connectivity are also examined.

The fullerenes are a class of threefold-coordinated molecules consisting of $\frac{n}{2}-10$ hexagons and 12 pentagons.[11] With increasing n their shape resembles more and more the honeycomb lattice, albeit in closed form, with the pentagons playing the role of structural impurities. Frustration decreases with n, as the unfrustrated hexagons dominate in number the frustrated pentagons while the distribution of the latter determines the symmetry group of the molecule. The properties of the AHM have been computed for the smallest element of the family, the dodecahedron, which consists only of pentagons and belongs to the icosahedral point symmetry group I_h. For classical spins the signature of frustration is very strong, generating three magnetization discontinuities in an external magnetic field, unexpectedly for a model lacking magnetic anisotropy.[8,12] In the full quantum limit where the individual spin magnitude $s_i=\frac{1}{2}$, the low-energy spectrum consists of singlets, absent in unfrustrated systems.[10] More unconventional behavior is displayed by the magnetization which is discontinuous in an external field as in the classical case, and the specific heat which has a two-peak structure as a function of temperature. For $s_i=1$ nonmagnetic excitations are still present inside the singlet-triplet gap, and now there are two magnetization discontinuities in a field. Similar behavior with magnetization discontinuities was also found for the AHM on larger fullerene molecules of I_h symmetry for classical and $s_i=\frac{1}{2}$ spins.[8] There is a strong evidence that this behavior is persistent for I_h symmetry in the $n\rightarrow\infty$ limit and survives asymptotically close to the zero and saturation fields, even though the number of hexagons strongly dominates the 12 frustrated pentagons.

Motivated by the nontrivial spectral and magnetic properties of the AHM on the I_h clusters, the $s_i=\frac{1}{2}$ AHM on

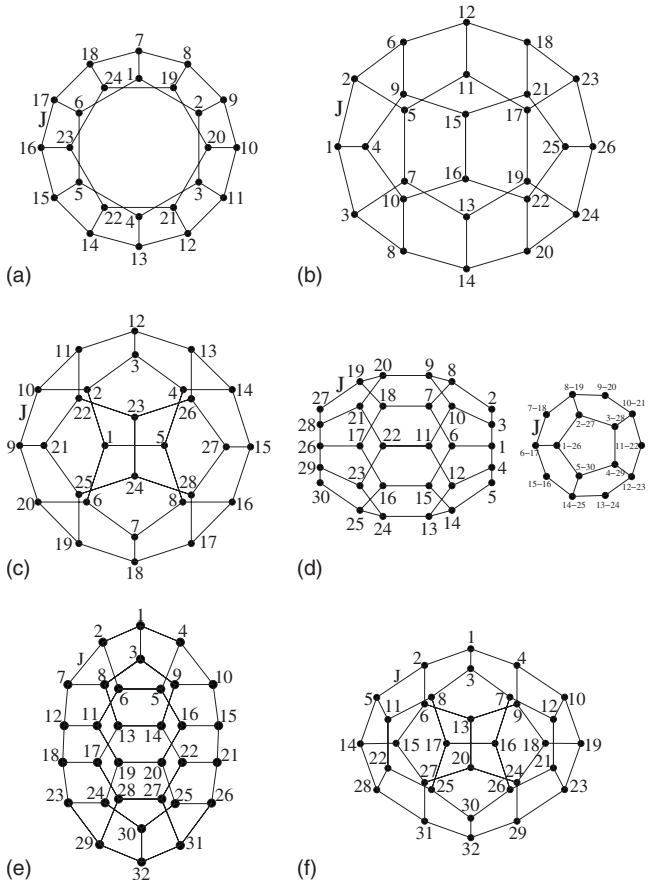

FIG. 1. Projection of the clusters on a plane: (a) C_{24}, (b) C_{26}, (c) C_{28}, (d) C_{30} (e) $C_{32,I}$, and (f) $C_{32,II}$. For C_{30} there is also a top (bottom with the dashes) view. The black circles are spins s_i. The solid lines are antiferromagnetic bonds J.

fullerene clusters with symmetry other than I_h is investigated. Modine and Kaxiras[13] calculated ground-state energies and correlation functions of clusters with n up to 28 and by truncating the Hilbert space of a cluster with $n=32$. They used no symmetries to reduce the computational requirements and found that same-hexagon correlations are the most important for the minimization of the energy. For the $n=28$ cluster more specifically the ground state was found to be doubly degenerate. Their results are extended here with the calculation of the low-energy excitations and the response in a magnetic field for the clusters of Ref. 13 with $n=24$ and 28. The magnetic behavior of different clusters with $n=26$ and 32 is investigated, as well as for a cluster with $n=30$. They are the most symmetric isomers for each n (for $n=32$ the two clusters belong to different point groups who have the same number of symmetry operations). They are abbreviated as C_n, with the D_{3d} $n=32$ cluster $C_{32,I}$, and the D_{3h} $n=32$ cluster $C_{32,II}$. All of them are shown in Fig. 1.[11,14] The spatial symmetry group along with the number of symmetry operations is listed in Table I for each n. The low-energy spectra are calculated with Lanczos diagonalization, and point-group and spin-inversion symmetries are used to reduce the computational requirements and to classify the states according to the total symmetry group's irreducible representations.[10] Similarly to the I_h-symmetry case it is of interest to look for nonmagnetic states inside the singlet-triplet gap, and search for unconventional behavior of the magnetization and the possible presence of discontinuities in a field. Comparing with the case of the I_h clusters we gauge the effect of symmetry on the behavior of the AHM on the fullerenes. It is noted that fullerene clusters are edge sharing and not corner sharing, and it is not obvious if it is possible to rewrite the Hamiltonian as a sum of total spins on individual units or how to perform any other mathematical operations in order to derive analytic results, even in the classical limit.

TABLE I. Symmetry and ground-state properties for the six clusters. $\frac{E_0}{n}$ is the ground-state energy per spin and mult. is the state's multiplicity. h_{sat} is the saturation field.

Sites n	Symmetry group	Number of symmetry operations	$\frac{E_0}{n}$	mult.	h_{sat}
24	D_{6d}	24	−0.48831	1	$4+\sqrt{2}$
26	D_{3h}	12	−0.48496	1	$4+\sqrt{2}$
28	T_d	24	−0.48482	2	$4+\sqrt{2}$
30	D_{5h}	20	−0.49625	1	$3+\sqrt{7}$
32 (I)	D_{3d}	12	−0.49597	1	$\frac{9+\sqrt{5}}{2}$
32 (II)	D_{3h}	12	−0.49804	1	5.61050

The plan of this paper is as follows: in Sec. II the model, method, and cluster structure are introduced, and in Sec. III the low-energy spectra and nearest-neighbor correlation functions are presented. Section IV presents the results on the ground-state magnetization and Sec. V presents the conclusions.

II. MODEL, METHOD, AND CLUSTER STRUCTURE

The antiferromagnetic Heisenberg Hamiltonian with spins $\vec{s}_i$ located on cluster vertices i is

$$H = J\sum_{\langle i,j\rangle} \vec{s}_i \cdot \vec{s}_j - hS^z, \tag{1}$$

where $\langle\ \rangle$ denotes nearest neighbors, and J is positive and will be set equal to 1 from now on, defining the unit of energy. h is the strength of an external magnetic field and S^z the projection of the total spin S along the field direction z. The Hamiltonian is diagonalized in all the irreducible representations generated by the symmetry group of each cluster to produce the eigenenergies and their corresponding wave functions.[10] Then by comparison of the low-energy spectra of the irreducible representations the full low-energy spectrum is constructed, where the ground state is the one with the minimal energy. The data for the symmetry groups was taken from Ref. 15. Degeneracies are reported with respect to states with specific S, each of which corresponds to $2S+1$ states with different value of S^z. For example, an expression of the form "k-times degenerate triplet" refers to a triplet ($S=1$, three states in total with $S^z=1,0,-1$, respectively), which is k-times degenerate due to spatial symmetry. Lanczos diagonalization was performed in double precision but

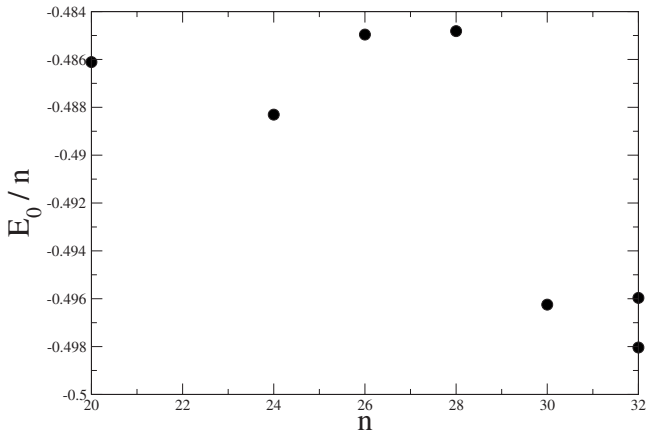

FIG. 2. Ground-state energy per spin $\frac{E_0}{n}$ as a function of the number of spins n. The value for $n=20$ is taken from Ref. 10. The lowest energy for $n=32$ is for cluster $C_{32,II}$ and the highest for $C_{32,I}$.

results are shown with a smaller number of significant digits to facilitate the presentation.

To calculate correlation functions $\langle \vec{s}_i \cdot \vec{s}_j \rangle$, where i and j could now be any two sites on the cluster, the wave functions are expanded back to the simple S^z basis $|k\rangle$ which is the product of up or down $\frac{1}{2}$ spins on individual sites. Each symmetry-adapted basis function is of the form

$$|\psi_j\rangle = \sum_k \alpha_k^j |k\rangle, \tag{2}$$

where the index j counts the states in a particular irreducible representation and α_k^j are, in general, complex coefficients. The wave functions are linear combinations of these states,

$$|\Psi_r\rangle = \sum_j \beta_j^r |\psi_j\rangle, \tag{3}$$

where r is the wave-function index and β_j^r complex coefficients. Then for state $|\Psi_r\rangle$,

$$\langle \vec{s}_i \cdot \vec{s}_j \rangle = \sum_l \beta_l^{r*} \sum_j \beta_j^r \sum_m \alpha_m^{l*} \sum_k \alpha_k^j \langle m | \vec{s}_i \cdot \vec{s}_j | k \rangle \tag{4}$$

which reduces to the calculation of the matrix elements $\langle m | \vec{s}_i \cdot \vec{s}_j | k \rangle$.

Sites which belong only to pentagons will be called pentagon sites while the rest hexagon sites. Looking at Fig. 1, the pentagons form a band in the middle of C_{24} while the hexagons a band in the middle of C_{30} and $C_{32,I}$. For C_{26} and C_{28} no hexagons are sharing edges while for $C_{32,II}$ the hexagons are adjacent to each other in two groups of three. Close proximity of polygons of the same kind can, in principle, minimize frustration, which also decreases on the average with n.

III. LOW-ENERGY SPECTRA AND CORRELATION FUNCTIONS

The ground-state energies per spin along with their degeneracies are listed in Table I. They are plotted as a function of n in Fig. 2. The bigger clusters with $n=30$ and 32 achieve the lowest energy while C_{26} and C_{28} the highest. C_{24} has the next lowest energy. Proximity of polygons of the same kind is crucial for energy minimization.[13] C_{26} and C_{28} do not have hexagons adjacent to each other (Fig. 1) and their energy per spin is even higher than the corresponding energy for the dodecahedron, which has no hexagons.[10] They show that increase in the number of hexagons does not necessarily lead to lower energy per spin. For C_{24} there is a band of pentagons separating the two hexagons. For the bigger clusters the hexagons approach each other more and more and lower the energy, with $C_{32,II}$ having the lowest. Its structure is such that there are two groups of three adjacent hexagons each [Fig. 1(f)] and all hexagon-hexagon bond correlations are strong (Table II). In addition, there is a set of three pentagon-pentagon bonds in the middle of the cluster that have a very strong singlet character with a correlation value equal to

TABLE II. Distinct nearest-neighbor correlation functions for the ground states.

Sites n	Intrahexagon	Interhexagon	Hexagon-pentagon	Intrapentagon
24	$\langle \vec{S}_1 \cdot \vec{S}_2 \rangle = -0.40325$		$\langle \vec{S}_1 \cdot \vec{S}_7 \rangle = -0.20285$	$\langle \vec{S}_7 \cdot \vec{S}_8 \rangle = -0.37051$
26	$\langle \vec{S}_5 \cdot \vec{S}_7 \rangle = -0.33858$	$\langle \vec{S}_{11} \cdot \vec{S}_{12} \rangle = -0.10317$	$\langle \vec{S}_2 \cdot \vec{S}_5 \rangle = -0.26523$	$\langle \vec{S}_1 \cdot \vec{S}_2 \rangle = -0.33215$
	$\langle \vec{S}_5 \cdot \vec{S}_{11} \rangle = -0.42436$			
28	$\langle \vec{S}_1 \cdot \vec{S}_2 \rangle = -0.35418$	$\langle \vec{S}_1 \cdot \vec{S}_5 \rangle = -0.23883$	$\langle \vec{S}_2 \cdot \vec{S}_3 \rangle = -0.30347$	
30	$\langle \vec{S}_6 \cdot \vec{S}_7 \rangle = -0.36221$		$\langle \vec{S}_1 \cdot \vec{S}_6 \rangle = -0.24081$	$\langle \vec{S}_1 \cdot \vec{S}_2 \rangle = -0.34618$
	$\langle \vec{S}_7 \cdot \vec{S}_{18} \rangle = -0.35466$			
32 (D_{3d})	$\langle \vec{S}_5 \cdot \vec{S}_6 \rangle = -0.37205$		$\langle \vec{S}_2 \cdot \vec{S}_6 \rangle = -0.30381$	$\langle \vec{S}_1 \cdot \vec{S}_2 \rangle = -0.30903$
	$\langle \vec{S}_5 \cdot \vec{S}_{16} \rangle = -0.32629$			
	$\langle \vec{S}_{11} \cdot \vec{S}_{12} \rangle = -0.24979$			
	$\langle \vec{S}_{11} \cdot \vec{S}_{19} \rangle = -0.45409$			
32 (D_{3h})	$\langle \vec{S}_1 \cdot \vec{S}_2 \rangle = -0.36273$	$\langle \vec{S}_{11} \cdot \vec{S}_{22} \rangle = -0.24352$	$\langle \vec{S}_5 \cdot \vec{S}_{14} \rangle = -0.16367$	$\langle \vec{S}_{14} \cdot \vec{S}_{15} \rangle = -0.60548$
	$\langle \vec{S}_2 \cdot \vec{S}_5 \rangle = -0.35602$			
	$\langle \vec{S}_5 \cdot \vec{S}_{11} \rangle = -0.41480$			

TABLE III. Low-energy spectrum for the six clusters. E is the energy, mult. stands for the multiplicity of the state, and irrep. for irreducible representation. S is the total spin, with each S state corresponding to $2S+1$ states with different projection of the total spin along the z axis S^z. The spatial irreducible representation notation follows Ref. 15. Indices s and a indicate the behavior under spin inversion, where s stands for symmetric and a for antisymmetric. A comma is introduced when necessary to avoid confusion between the notation for the spatial irreducible representation and the behavior under spin inversion.

C_{24}				C_{26}				C_{28}			
E	mult.	irrep.	S	E	mult.	irrep.	S	E	mult.	irrep.	S
−11.71937	1	$B_{1,s}$	0	−12.60898	1	$A'_{2,a}$	0	−13.57486	2	E_s	0
−11.70478	1	$A_{1,s}$	0	−12.55739	2	E'_a	0	−13.55978	3	$T_{2,a}$	1
−11.46814	2	$E_{3,a}$	1	−12.49297	2	E'_s	1	−13.50468	3	$T_{2,s}$	0
−11.37244	1	$A_{2,a}$	1	−12.46174	1	$A''_{2,a}$	0	−13.49099	2	E_s	0
−11.29779	1	$B_{1,s}$	0	−12.44862	1	$A''_{2,a}$	0	−13.42327	1	$A_{1,s}$	2
−11.29326	2	$E_{2,s}$	0	−12.42682	2	E'_a	0	−13.38652	2	E_a	1
−11.27888	1	$B_{2,a}$	1	−12.42129	2	E'_s	1	−13.36105	3	$T_{2,a}$	1
−11.26341	2	$E_{5,a}$	1	−12.38217	1	$A'_{1,s}$	1	−13.29319	3	$T_{1,s}$	0
−11.24565	2	$E_{5,s}$	0	−12.37889	1	$A''_{1,s}$	1	−13.27818	3	$T_{1,a}$	1
−11.23652	2	$E_{2,a}$	1	−12.31502	1	$A'_{2,a}$	0	−13.22866	3	$T_{2,a}$	1
−11.23043	1	$A_{1,s}$	0	−12.30577	2	E''_s	1	−13.21762	1	$A_{1,s}$	0
−11.22852	2	$E_{1,a}$	1	−12.28884	2	E'_s	1	−13.19914	3	$T_{2,s}$	0
−11.17883	2	$E_{3,a}$	1	−12.26375	2	E''_a	0	−13.19486	3	$T_{1,a}$	1
−11.16437	2	$E_{4,s}$	0	−12.21057	1	$A'_{1,s}$	1	−13.18471	2	E_s	0
−11.16257	2	$E_{1,s}$	0	−12.16192	2	E''_s	1	−13.17446	3	$T_{2,a}$	1
−11.15826	2	$E_{3,s}$	0	−12.15183	2	$A''_{1,a}$	0	−13.14963	1	$A_{2,s}$	0
−11.13896	2	$E_{4,a}$	1	−12.14598	2	E'_s	1	−13.14309	1	$A_{1,a}$	1
−11.05126	1	$A_{1,s}$	0	−12.13819	1	$A'_{2,a}$	2	−13.11265	3	$T_{2,s}$	2

C_{30}				$C_{32,I}$				$C_{32,II}$			
E	mult.	irrep.	S	E	mult.	irrep.	S	E	mult.	irrep.	S
−14.88742	1	$A''_{2,a}$	0	−15.87092	1	$A_{1u,s}$	0	−15.93723	1	$A''_{1,s}$	0
−14.83815	2	$E''_{2,a}$	0	−15.81199	2	$E_{g,s}$	0	−15.81192	2	E'_s	0
−14.82517	1	$A'_{2,a}$	0	−15.80648	1	$A_{1g,s}$	0	−15.77366	1	$A'_{2,a}$	1
−14.62495	1	$A'_{1,s}$	1	−15.67299	2	$E_{u,a}$	1	−15.73368	1	$A'_{1,s}$	0
−14.60458	2	$E'_{2,s}$	1	−15.59634	2	$E_{g,a}$	1	−15.63730	2	E'_a	1
−14.59928	1	$A''_{1,s}$	1	−15.57987	1	$A_{2u,a}$	1	−15.60167	2	E'_a	1
−14.51907	2	$E'_{1,s}$	1	−15.52875	2	$E_{g,s}$	0	−15.57485	2	E''_s	0
−14.50190	2	$E''_{1,a}$	0	−15.51890	1	$A_{1g,s}$	0	−15.56589	2	E''_a	1
−14.48316	2	$E'_{2,s}$	1	−15.49978	2	$E_{u,a}$	1	−15.54070	2	E''_a	1
−14.47476	1	$A''_{2,a}$	0	−15.49168	1	$A_{2g,a}$	1	−15.50045	1	$A''_{2,a}$	1
−14.46287	2	$E''_{2,s}$	1	−15.47080	1	$A_{1u,s}$	0	−15.49288	1	$A''_{1,s}$	0
−14.45130	2	$E''_{1,s}$	1	−15.46339	1	$A_{1u,a}$	1	−15.46219	1	$A''_{1,s}$	0
−14.33694	2	$E'_{1,a}$	0	−15.45531	2	$E_{g,a}$	1	−15.45437	1	$A'_{2,a}$	1
−14.27711	2	$E''_{1,a}$	0	−15.44665	2	$E_{u,s}$	0	−15.45317	1	$A'_{1,a}$	1
−14.26727	1	$A'_{2,a}$	0	−15.44513	2	$E_{g,a}$	1	−15.42185	2	E''_s	0
−14.23932	1	$A'_{1,s}$	1	−15.43356	1	$A_{2g,a}$	1	−15.39363	1	$A''_{2,a}$	1
−14.17268	2	$E''_{2,s}$	1	−15.38287	1	$A_{1g,s}$	2	−15.38231	1	$A''_{2,a}$	1
−14.16221	1	$A'_{2,a}$	2	−15.38034	1	$A_{2u,a}$	1	−15.38020	2	E''_a	1

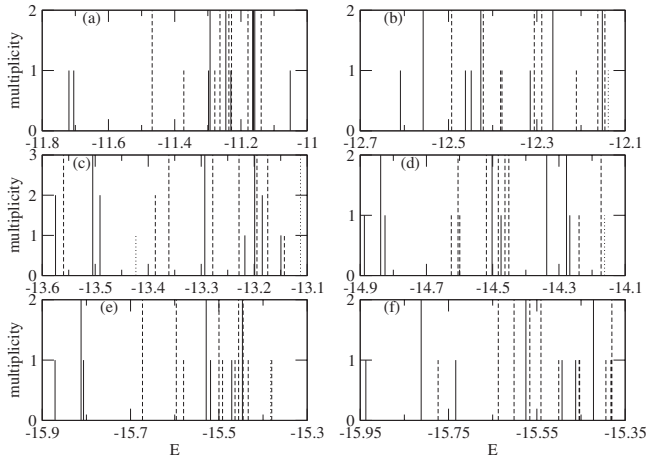

FIG. 3. Low-energy E spectrum of total spin S states and its multiplicity: (a) C_{24}, (b) C_{26}, (c) C_{28}, (d) C_{30} (e) $C_{32,I}$, and (f) $C_{32,II}$. Solid lines: $S=0$, dashed lines: $S=1$, and dotted lines: $S=2$.

−0.60548. Such a strong correlation is not achieved even within hexagons in any of the clusters and points to the importance of the specific structure geometry rather than the symmetry for the minimization of the energy, at least for the fullerene clusters with small n considered in this paper. The two hexagon groups and the strong singletlike pentagon bonds are correlated weakly with the rest of the spins. Apart from $C_{32,II}$, the dominant nearest-neighbor correlations in the ground state are of the intrahexagon type, with intrapentagon following closely (Table II).

The low-energy spectra are shown in Table III and Fig. 3. Frustration results in nonmagnetic excitations inside the singlet-triplet gap. Except from C_{28} the ground and first-excited states are singlets, with the ground states nondegenerate and the first-excited states doubly degenerate, except from C_{24} where it is nondegenerate. For C_{30} and $C_{32,I}$ the second excited state is also a nondegenerate singlet. As seen in Figs. 3(d) and 3(e) the low-energy spectra of C_{30} and $C_{32,I}$ are similar. There is a nondegenerate singlet followed by two closely spaced singlets with the same degeneracy. In addition, as with C_{24}, the low-lying singlets are well separated from the magnetic excitations. The two clusters belong to different symmetry groups but they both have their hexagons forming a band in the middle. Spin-inversion symmetry is however opposite for the six lowest states in the spectra (Table III). C_{26} and $C_{32,II}$ on the other hand have the same spatial symmetry, D_{3h}. In their low-energy spectra the ground states belong to different irreducible representations and their spin-inversion symmetry is also different. The first-excited states belong to the same irreducible representation, however the spin-inversion symmetry is still different. This is in contrast to the smallest dodecahedral I_h-symmetry clusters, the icosahedron (not of the fullerene type and made only of triangles) and the dodecahedron, which have similar structure and relative spacing of the levels in their low-energy spectra even though they comprise of different polygons, therefore symmetry is a strong determining factor for their properties. This result points to the conclusion that spatial symmetry is not the only factor determining the low-energy properties, in general, for the fullerenes.

TABLE IV. Distinct nearest-neighbor correlation functions for the singlet excited states within the singlet-triplet gap.

Sites n	Intrahexagon	Interhexagon	Hexagon-pentagon	Intrapentagon
24	$\langle\vec{S}_1\cdot\vec{S}_2\rangle=-0.37785$		$\langle\vec{S}_1\cdot\vec{S}_7\rangle=-0.25586$	$\langle\vec{S}_7\cdot\vec{S}_8\rangle=-0.34169$
26	$\langle\vec{S}_5\cdot\vec{S}_7\rangle=-0.28615$	$\langle\vec{S}_{11}\cdot\vec{S}_{12}\rangle=-0.084111$	$\langle\vec{S}_2\cdot\vec{S}_5\rangle=-0.30251$	$\langle\vec{S}_1\cdot\vec{S}_2\rangle=-0.30687$
	$\langle\vec{S}_5\cdot\vec{S}_{11}\rangle=-0.42640$			
30	$\langle\vec{S}_6\cdot\vec{S}_7\rangle=-0.37609$		$\langle\vec{S}_1\cdot\vec{S}_6\rangle=-0.21102$	$\langle\vec{S}_1\cdot\vec{S}_2\rangle=-0.35548$
	$\langle\vec{S}_7\cdot\vec{S}_{18}\rangle=-0.33026$			
30	$\langle\vec{S}_6\cdot\vec{S}_7\rangle=-0.37784$		$\langle\vec{S}_1\cdot\vec{S}_6\rangle=-0.20832$	$\langle\vec{S}_1\cdot\vec{S}_2\rangle=-0.35598$
	$\langle\vec{S}_7\cdot\vec{S}_{18}\rangle=-0.32507$			
32 (D_{3d})	$\langle\vec{S}_5\cdot\vec{S}_6\rangle=-0.39744$		$\langle\vec{S}_2\cdot\vec{S}_6\rangle=-0.30566$	$\langle\vec{S}_1\cdot\vec{S}_2\rangle=-0.29805$
	$\langle\vec{S}_5\cdot\vec{S}_{16}\rangle=-0.29843$			
	$\langle\vec{S}_{11}\cdot\vec{S}_{12}\rangle=-0.27220$			
	$\langle\vec{S}_{11}\cdot\vec{S}_{19}\rangle=-0.45947$			
32 (D_{3d})	$\langle\vec{S}_5\cdot\vec{S}_6\rangle=-0.40407$		$\langle\vec{S}_2\cdot\vec{S}_6\rangle=-0.29314$	$\langle\vec{S}_1\cdot\vec{S}_2\rangle=-0.30482$
	$\langle\vec{S}_5\cdot\vec{S}_{16}\rangle=-0.30669$			
	$\langle\vec{S}_{11}\cdot\vec{S}_{12}\rangle=-0.27231$			
	$\langle\vec{S}_{11}\cdot\vec{S}_{19}\rangle=-0.45357$			
32 (D_{3h})	$\langle\vec{S}_1\cdot\vec{S}_2\rangle=-0.36028$	$\langle\vec{S}_{11}\cdot\vec{S}_{22}\rangle=-0.16865$	$\langle\vec{S}_5\cdot\vec{S}_{14}\rangle=-0.24184$	$\langle\vec{S}_{14}\cdot\vec{S}_{15}\rangle=-0.40508$
	$\langle\vec{S}_2\cdot\vec{S}_5\rangle=-0.34068$			
	$\langle\vec{S}_5\cdot\vec{S}_{11}\rangle=-0.41156$			

TABLE V. Distinct nearest-neighbor correlation functions for the first triplet excited states.

Sites n	Intrahexagon	Interhexagon	Hexagon-pentagon	Intrapentagon
24	$\langle\vec{S}_1\cdot\vec{S}_2\rangle=-0.38523$		$\langle\vec{S}_1\cdot\vec{S}_7\rangle=-0.20358$	$\langle\vec{S}_7\cdot\vec{S}_8\rangle=-0.36686$
26	$\langle\vec{S}_5\cdot\vec{S}_7\rangle=-0.34294$	$\langle\vec{S}_{11}\cdot\vec{S}_{12}\rangle=-0.13733$	$\langle\vec{S}_2\cdot\vec{S}_5\rangle=-0.25900$	$\langle\vec{S}_1\cdot\vec{S}_2\rangle=-0.33365$
	$\langle\vec{S}_5\cdot\vec{S}_{11}\rangle=-0.40945$			
28	$\langle\vec{S}_1\cdot\vec{S}_2\rangle=-0.32073$	$\langle\vec{S}_1\cdot\vec{S}_5\rangle=-0.22540$	$\langle\vec{S}_2\cdot\vec{S}_3\rangle=-0.33309$	
	$\langle\vec{S}_4\cdot\vec{S}_5\rangle=-0.42032$	$\langle\vec{S}_{10}\cdot\vec{S}_{11}\rangle=-0.010665$	$\langle\vec{S}_3\cdot\vec{S}_4\rangle=-0.16012$	
	$\langle\vec{S}_2\cdot\vec{S}_{10}\rangle=-0.42541$			
30	$\langle\vec{S}_6\cdot\vec{S}_7\rangle=-0.35985$		$\langle\vec{S}_1\cdot\vec{S}_6\rangle=-0.22022$	$\langle\vec{S}_1\cdot\vec{S}_2\rangle=-0.34857$
	$\langle\vec{S}_7\cdot\vec{S}_{18}\rangle=-0.34801$			
32 (D_{3d})	$\langle\vec{S}_5\cdot\vec{S}_6\rangle=-0.40953$		$\langle\vec{S}_2\cdot\vec{S}_6\rangle=-0.25415$	$\langle\vec{S}_1\cdot\vec{S}_2\rangle=-0.32989$
	$\langle\vec{S}_5\cdot\vec{S}_{16}\rangle=-0.33089$			
	$\langle\vec{S}_{11}\cdot\vec{S}_{12}\rangle=-0.28203$			
	$\langle\vec{S}_{11}\cdot\vec{S}_{19}\rangle=-0.42064$			
32 (D_{3h})	$\langle\vec{S}_1\cdot\vec{S}_2\rangle=-0.35863$	$\langle\vec{S}_{11}\cdot\vec{S}_{22}\rangle=-0.24266$	$\langle\vec{S}_5\cdot\vec{S}_{14}\rangle=-0.15494$	$\langle\vec{S}_{14}\cdot\vec{S}_{15}\rangle=-0.61209$
	$\langle\vec{S}_2\cdot\vec{S}_5\rangle=-0.35762$			
	$\langle\vec{S}_5\cdot\vec{S}_{11}\rangle=-0.40890$			

C_{28} differs from the rest of the clusters in that its ground state is a doubly degenerate singlet[13] while the first-excited state is a closely spaced triply degenerate triplet (Table III). Then triply and doubly degenerate singlets follow, and the first nondegenerate state which has $S=2$. In no other cluster an $S=2$ state lies so low in the excitation spectrum. The ground-state doublet belongs to the E_s representation, which transforms as the pair $(x^2-y^2, 2z^2-x^2-y^2)$ of Cartesian tensors.[15] In contrast to Ref. 13, here we find the correlations to be the same for both degenerate ground states.

The nearest-neighbor correlation functions for the lowest singlet excitations are listed in Table IV. The two smallest clusters and $C_{32,II}$ lower the energy of the hexagon-pentagon bonds while increasing the energy of the rest (only one of the same-hexagon bonds of C_{26} lowers very weakly). On the contrary, C_{30} behaves the other way, except from the intrahexagon correlation in the middle of the cluster that refers to a common side of two hexagons, which weakens. Its two singlet excited states are very close in energy and in the behavior of the correlation functions, even though they are of different multiplicity, which is also true for $C_{32,I}$. The latter alters its same-hexagon bonds to generate the two excited singlets, even though the strongest one that refers to a common side of two hexagons does not change significantly.

The nearest-neighbor correlation functions for the first triplet excitation are shown in Table V. The values for $C_{32,II}$

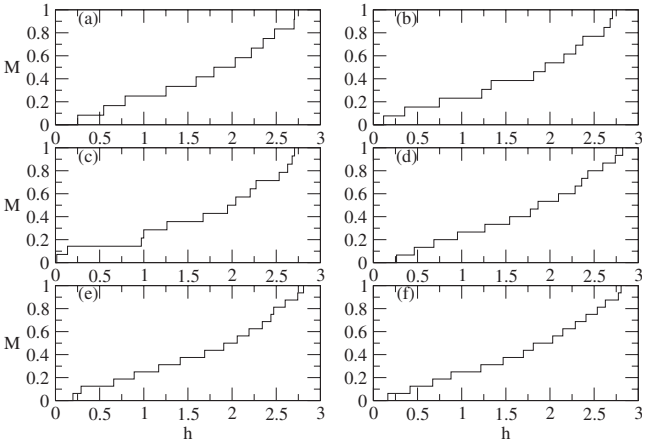

FIG. 4. Reduced ground-state magnetization $M=\frac{S}{ns_i}$ as a function of magnetic field h: (a) C_{24}, (b) C_{26}, (c) C_{28}, (d) C_{30}, (e) $C_{32,I}$, and (f) $C_{32,II}$. M is the total spin S normalized to the number of sites n and the magnitude of spin s_i. M has no units and h is in units of energy.

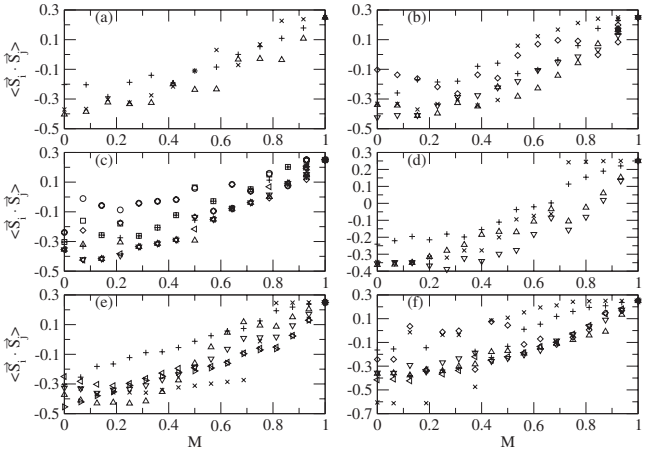

FIG. 5. Distinct correlation functions for the lowest-energy state in each total spin S sector: (a) C_{24}, (b) C_{26}, (c) C_{28}, (d) C_{30}, (e) $C_{32,I}$, and (f) $C_{32,II}$. The reduced magnetization $M=\frac{S}{ns_i}$ is the total spin S normalized to the number of sites n and the magnitude of spin s_i. $\langle\vec{S}_i\cdot\vec{S}_j\rangle$ is in units of energy and M has no units. $\langle\vec{S}_i\cdot\vec{S}_j\rangle$: $\triangle$, $\triangleleft$, $\triangleright$, $\triangledown$: intrahexagon, $\diamond$, $\bigcirc$: interhexagon, +, $\square$: hexagon-pentagon, and $\times$: intrapentagon.

TABLE VI. Lowest energies (E_0), multiplicities (mult.), and corresponding irreducible representations (irrep.) in each total spin S sector for the clusters. The spatial irreducible representation notation follows Ref. 15. Indices s and a indicate the behavior under spin inversion, where s stands for symmetric and a for antisymmetric. It is only possible to calculate them for states lying relatively low or high in the energy spectrum. A comma is introduced when necessary to avoid confusion between the notation for the spatial irreducible representation and the behavior under spin inversion.

	C_{24}			C_{26}			C_{28}		
S	E_0	mult.	irrep.	E_0	mult.	irrep.	E_0	mult.	irrep.
0	−11.71937	1	$B_{1,s}$	−12.60898	1	$A'_{2,a}$	−13.57486	2	E_s
1	−11.46814	2	$E_{3,a}$	−12.49297	2	E'_s	−13.55978	3	$T_{2,a}$
2	−10.92259	1	$B_{1,s}$	−12.13819	1	$A'_{2,a}$	−13.42327	1	$A_{1,s}$
3	−10.13390	1	$B_{2,a}$	−11.39120	1	$A'_{1,s}$	−12.45085	3	$T_{2,a}$
4	−8.88178	1	$A_{1,s}$	−10.16420	1	$A'_{2,a}$	−11.45102	1	$A_{1,s}$
5	−7.28948	2	E_5	−8.83042	1	$A'_{1,s}$	−10.18889	1	$A_{1,a}$
6	−5.49575	1	A_1	−7.01596	1	A'_2	−8.51700	1	A_1
7	−3.46016	1	B_2	−5.07125	1	A'_1	−6.56848	3	T_2
8	−1.24214	1	B_1	−2.91337	2	E'	−4.52626	2	E
9	1.10955	1	A_2	−0.62134	2	E'	−2.32108	1	A_1
10	3.59067	1	$B_{1,s}$	1.75066	1	A'_2	−0.049533	1	A_1
11	6.29289	2	$E_{3,a}$	4.36198	1	A'_1	2.48354	3	T_2
12	9	1	$A_{1,s}$	7.04289	1,2	$A'_{2,a}, E'$	5.11292	2	E
13				9.75	1	$A'_{1,s}$	7.79289	1,3	$A_{1,a}, T_2$
14							10.5	1	$A_{1,s}$

	C_{30}			$C_{32,I}$			$C_{32,II}$		
S	E_0	mult.	irrep.	E_0	mult.	irrep.	E_0	mult.	irrep.
0	−14.88742	1	$A''_{2,a}$	−15.87092	1	$A_{1u,s}$	−15.93723	1	$A''_{1,s}$
1	−14.62495	1	$A'_{1,s}$	−15.67299	2	$E_{u,a}$	−15.77366	1	$A'_{2,a}$
2	−14.16221	1	$A'_{2,a}$	−15.38287	1	$A_{1g,s}$	−15.35876	1	A'_1
3	−13.47738	2	$E'_{2,s}$	−14.72334	1	A_{2g}	−14.68665	1	A'_2
4	−12.52542	1	A''_2	−13.83231	1	A_{1g}	−13.80765	1	A'_1
5	−11.26275	1	A''_1	−12.66407	1	A_{2g}	−12.59064	1	A'_1
6	−9.71967	2	E''_2	−11.25111	1	A_{1g}	−11.12132	1	A''_1
7	−7.94218	2	E'_2	−9.56173	1	A_{2g}	−9.42233	1	A'_1
8	−6.07738	1	A''_2	−7.65604	1	A_{1g}	−7.61188	1	A'_1
9	−3.98134	1	A''_1	−5.59828	1	A_{2g}	−5.58108	1	A''_2
10	−1.69706	1	A'_2	−3.40688	1	A_{1g}	−3.43626	1	A'_1
11	0.66164	1	A'_1	−1.06488	1	A_{2g}	−1.14953	1	A''_2
12	3.08988	1	A''_2	1.37454	1	A_{2g}	1.25805	1	A'_1
13	5.68792	1	A'_1	3.84610	1	A_{2g}	3.79378	1	A''_2
14	8.42712	1	A''_2	6.44732	1	A_{1g}	6.42049	1	A'_1
15	11.25	1	$A'_{1,s}$	9.19098	1	A_{2g}	9.19475	1	A''_2
16				12	1	$A_{1g,s}$	12	1	$A'_{1,s}$

change relatively little compared to the ground state, and the pentagon-pentagon correlation is getting even stronger. Similarly, C_{30} shows little change except from the hexagon-pentagon correlation that gets weaker. For C_{24} the triplet is mostly due to the decrease in the intrahexagon correlation function while in C_{26} the interhexagon correlation is getting stronger. In C_{28} only the interhexagon correlation $\langle \vec{S}_1 \cdot \vec{S}_5 \rangle$ changes relatively weakly compared to the other correla-

tions, and correlation $\langle \vec{S}_{10} \cdot \vec{S}_{11} \rangle$ is particularly weak. Finally, for $C_{32,I}$ there are strong changes for all correlations except from $\langle \vec{S}_5 \cdot \vec{S}_{16} \rangle$.

IV. GROUND-STATE MAGNETIZATION

The ground-state magnetization as a function of an external field has typically a steplike structure, with a $\Delta S=1$ discontinuity at fields where the ground state switches between adjacent S sectors. Frustration though can lead to magnetization discontinuities with $\Delta S>1$, where a particular S sector never becomes the ground state in a field. Such is the case for the icosahedral symmetry I_h clusters, where the sector $S=\frac{n}{2}-5$ with five flipped spins from saturation never includes the ground state.[8] The number of discontinuities is more than one at the classical level $S \to \infty$, and also for the dodecahedron ($n=20$) and $s_i=1$, where the calculation of the lowest-energy state is computationally feasible for all S sectors (for I_h clusters with $n>20$ the lowest-energy state calculation is only possible for very high S even for $s_i=\frac{1}{2}$).

The lowest states for all the S sectors along with their degeneracies and the irreducible representation to which they belong are listed in Table VI (the saturation fields are listed in Table I). The corresponding reduced magnetization $M=\frac{S}{ns_i}$ curves are shown in Fig. 4. Unlike the icosahedral symmetry case, no discontinuities are found. For some values of M there are plateaux, where a particular S sector contains the ground state for a wider range of fields than the neighboring sectors. The most pronounced appears for C_{28} and $S=2$, where $M=0.14286$ [Fig. 4(c)]. It is again hard to draw correlations between symmetry and the response in a magnetic field. In Figs. 4(a) and 5(a) there is a correlation of the plateaulike features of the magnetization curve of C_{24} with stronger values of the intrahexagon bonds. For C_{28}, where the singlet-triplet gap is very small, there are stronger intrahexagon correlation functions for the few low-lying $S>0$ sectors compared to the singlet case [Fig. 5(c)]. There are S sectors that contain the ground state for a very narrow range of the field [Fig. 4(c)], and looking at Table VI their lowest state belongs to three-dimensional irreducible representations. For C_{30}, sectors $S=3$ and 4 have very strong same-hexagon correlations, stronger than the ones in the ground state [Fig. 5(d)]. For $C_{32,I}$ there are strong same-hexagon correlations for the low-S sectors but for higher S intrapentagon correlations are the strongest [Fig. 5(e)]. In both cases, the strength of these correlations does not change significantly with the S value. $S=12$ is the first sector that restores the same-hexagon correlations as the strongest, and it is the ground state for a narrow field window [Fig. 4(e)]. In the case of $C_{32,II}$ there are low-S sectors where the intrapentagon correlation is very strong [Fig. 5(f)]. For $S=1$ and 3 it is even stronger than the $S=0$ value. For C_{26} the $S=4$ and 6 sectors are ground states for a narrow range of the field [Fig. 4(b)] and same-hexagon correlations are weak [Fig. 5(b)]. Finally, for C_{24} the single spin-flip subspace has the ground state for a very narrow window of the field [Fig. 4(a)], with the two spin-flip subspace having a plateau and the strongest intrahexagon correlations relative to its neighboring S sectors [Fig. 5(a)].

For C_{26} and C_{28} the sector with a single spin flip from saturation is degenerate (Table VI). However, the spin flips are not confined on the hexagons except from the singly degenerate state of C_{26}, therefore there is no analog with the high magnetization localized magnon states discussed in Ref. 16.

V. CONCLUSIONS

The low-energy spectrum and the magnetic response of the $s_i=\frac{1}{2}$ AHM have been calculated on a series of clusters with the connectivity of the fullerenes and a number of sites ranging from 24 to 32. Frustration and connectivity have a signature on the low-energy spectrum with singlet ground and low-energy excited states, the only exception being the 28-site cluster where the ground state is a doubly degenerate singlet and the first-excited state is a triplet. Frustration is minimal when pentagons and hexagons minimize their interference in the clusters by being placed adjacent to polygons of the same kind. The magnetization as a function of an external field exhibits plateaux features, the most pronounced for $n=28$ and $S=2$. The clusters considered in this paper have relatively small n and mostly belong to different spatial symmetry groups. Only C_{26} and $C_{32,II}$ share the same spatial symmetry, nevertheless they have no common pattern of low energy and magnetic behavior as was the case for I_h symmetry.[8,10] Similarities are only found in the low-energy behavior of C_{30} and $C_{32,I}$ even though they belong to different symmetry groups, and they have in common all the hexagons forming a band in the middle. It is also pointed out that there are some minor differences between type I and type II molecules as they were called in Ref. 8, even though they share the icosahedral I_h symmetry. Larger clusters can shed light on the magnetic properties as a function of the distribution of the pentagons, however present day computational means impose limitations, at least for the calculation of the low-energy properties. Nevertheless, connectivity appears to be as important as spatial symmetry for the magnetic properties, unlike the icosahedral I_h-symmetry clusters. For low n the competition between unfrustrated hexagons and frustrated pentagons is strong but even for high n the pentagon influence can be important, as in the case of I_h symmetry.[8]

ACKNOWLEDGMENT

The author thanks D. Coffey for discussions.

[1] G. Misguich and C. Lhuillier, in *Frustrated Spin Systems*, edited by H. T. Diep (World Scientific, Singapore, 2003).
[2] C. Lhuillier and P. Sindzingre, in *Quantum Properties of Low-Dimensional Antiferromagnets*, edited by Y. Ajiro and J. P. Boucher (Kyushu University Press, Fukuoka, Japan, 2002).
[3] C. Lhuillier and G. Misguich, in *High Magnetic Fields Applications in Condensed Matter Physics and Spectroscopy*, Lecture Notes in Physics (Springer Series) Vol. 595, edited by C. Berthier, L. P. Levy, and G. Martinez (Springer, New York, 2001).
[4] J. Schnack, Lect. Notes Phys. **645**, 155 (2004).
[5] A. F. Hebard, M. J. Roseeinsky, R. C. Haddon, D. W. Murphy, S. H. Glarum, T. T. M. Palstra, A. P. Ramirez, and A. R. Kortan, Nature (London) **350**, 600 (1991).
[6] K. Holczer, O. Klein, S.-M. Huang, R. B. Kaner, K.-J. Fu, R. L. Whetten, and F. Diederich, Science **252**, 1154 (1991).
[7] S. Chakravarty, M. Gelfand, and S. Kivelson, Science **254**, 970 (1991).
[8] N. P. Konstantinidis, Phys. Rev. B **76**, 104434 (2007).
[9] F. Lin, E. S. Sørensen, C. Kallin, and A. J. Berlinsky, Phys. Rev. B **76**, 033414 (2007).
[10] N. P. Konstantinidis, Phys. Rev. B **72**, 064453 (2005).
[11] P. W. Fowler and D. E. Manolopoulos, *An Atlas of Fullerenes* (Oxford University Press, New York, 1995).
[12] D. Coffey and S. A. Trugman, Phys. Rev. Lett. **69**, 176 (1992).
[13] N. A. Modine and E. Kaxiras, Phys. Rev. B **53**, 2546 (1996).
[14] M. Yoshida, http://cochem2.tutkie.tut.ac.jp:8000/Fuller/
[15] S. L. Altmann and P. Herzig, *Point-Group Theory Tables* (Oxford University Press, New York, 1994).
[16] J. Schulenburg, A. Honecker, J. Schnack, J. Richter, and H.-J. Schmidt, Phys. Rev. Lett. **88**, 167207 (2002).